Langmuir

Article

pubs.acs.org/Langmuir

Powerful Surface Chemistry Approach for the Grafting of Alkyl Multilayers on Aluminum Nanoparticles

Morgan Fogliazza, Lorette Sicard, Philippe Decorse, Alexandre Chevillot-Biraud, Claire Mangeney, and Jean Pinson*

Sorbonne Paris Cité, Interfaces, Traitements, Organisation et Dynamique des Systèmes (ITODYS), UMR 7086 CNRS, Université Paris Diderot, 15 rue J-A de Baïf, 75013 Paris, France

Supporting Information

ABSTRACT: The synthesis of aluminum nanoparticles (Alnp) has raised promising perspectives these past few years for applications in energetic materials. However, because of their high reactivity, it is crucial to functionalize them before their use. In this work, we propose an original and simple chemical approach to graft spontaneously alkyl layers derived from alkyl halides at the surface of Alnp, by relying on the highly reductive character of these nanoparticles, when they are in the unoxidized form. Alnp were prepared in a glovebox and reacted with alkyl halides (RI and RBr) to give modified Alnp−R, as shown by infrared spectroscopy (IR), X-ray photoelectron spectroscopy (XPS), X-ray diffraction, thermogravimetric analysis (TGA), and microscopy. The coating is made of alkyl multilayers, which were found to be strongly anchored at the Alnp surface, as it resisted 2 h of rinsing in toluene. An electrocatalytic electron transfer promoted by Alnp is proposed to describe the mechanism of this grafting reaction.

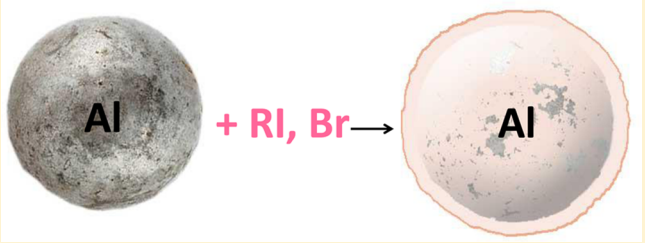

1. INTRODUCTION

Aluminum is a highly energetic material with a heat release during its burning of more than 30 kJ/g of Al (the heat of formation of Al_2O_3 is ΔH_f = 1669 kJ mol^{-1} at 298 K[1]). However, the rate of this combustion is relatively low and most often incomplete. To overcome this limitation, the use of reactive nanoparticles or nanocomposite powders has been proposed. Indeed, it has been shown that their small size and enhanced surface/volume ratio can increase the rate of aluminum burning and, thus, the overall reaction rate of energetic formulations[2−4] incorporating this material. Aluminum nanoparticles (Alnp) have, therefore, been considered as additives in propellants[5−7] for engines[8] and for rockets.[9] Nevertheless, there are three important concerns when using small Alnp with a high surface/volume ratio: (i) their strong tendency to spontaneously oxidize, leading to a partial loss of their energetic properties, (ii) their pyrophoric properties and high reactivity, which makes them difficult to manipulate, and (iii) their tendency to aggregate.

Coating of Alnp is a strategy addressing these issues, and it has been achieved by various ways, such as the grafting of carboxylic acids (perfluorocarboxylic acid[10] or oleic acid[11]), their coating with epoxyhexane (through the nucleophilic attack of Al on the epoxy groups),[12] or by combining the diazonium chemistry[13] on the surface of Alnp with the iniferter photochemical growth of a poly(methacrylic acid) film.[14] With carboxylic acids, a bridge bonding the carboxylate to the Al surface was observed,[10] while with diazonium salts, a radical attack on the surface of Al, partially oxidized, is deemed responsible for the formation of Al−O−C bonds. The main advantage of such a radical mechanism is the formation of compact multilayers of aryl groups, which were shown to promote the passivation of the Alnp surface and protect it efficiently from oxidation by air. However, one major drawback of the diazonium salts is their poor solubility in usual apolar organic solvent (such as ether, toluene, etc.), which limits their scope of applications. This is particularly a problem for aluminum because it is generally obtained from aluminum hydride, which reacts spontaneously in the presence of protons.

As an alternative to diazonium salts, alkyl halides have recently been proposed for the modification of metallic surfaces, in organic solvent. Modification of surfaces by alkyl halides can be achieved by two different types of experimental methods (see Scheme 1). The first one (reductive mechanism) involves a radical-based approach relying on the reduction of alkyl iodides and alkyl bromides. In the case of an electrochemical reduction, alkyl layers have been shown to be efficiently electrografted on metals[15] and carbon[16,17] at quite negative potentials [< −2.3 V/saturated calomel electrode (SCE)].

More positive potentials were sufficient on Cu,[15] Pd,[18,19] and Ag[20,21] (−1.3, −1.8, −1.1 V/SCE, respectively) because of an electrocatalysis phenomenon or on carbon in the presence of 2,6-dimethylbenzenediazonium thanks to a radical crossover reaction.[22] The general mechanism of the electrografting reactions involves the formation of an alkyl radical that reacts

Received: April 2, 2015
Revised: May 12, 2015
Published: May 14, 2015

DOI: 10.1021/acs.langmuir.5b01213
Langmuir 2015, 31, 6092−6098

Scheme 1. Two Possible Mechanisms for the Grafting of Alkyl Halides on Surfaces

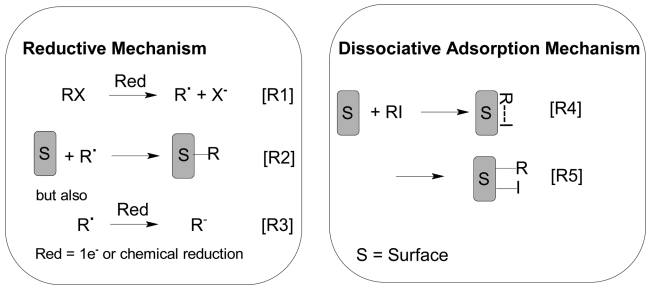

with the surface,[23] in competition with its further reduction to a carbanion. Strongly attached disordered mono- or multilayers are obtained by this method, with the interaction between the grafted alkyl films and the metallic surface being very stable. The stability of the grafted organic layer relies on the formation of a carbon−metal covalent bond and drives the examination of alkyl-halide-derived layers as an alternative to self-assembled monolayers for applications where extremely stable surface chemistry is required.

The second type of reaction (dissociative adsorption mechanism) is based on the dissociative chemisorption of alkyl halides on metallic surfaces, including Cu(110), Ag(111 and 110), Al(111 and 100), under ultra-high vacuum (UHV).[24] For example,[25−27] 1-iodo or 1-iodo 2-methylpropane undergo a C−I bond scission of the molecularly adsorbed 1-iodopropane and adsorption of propyl groups and iodine on the surface. The fact that the metal−C bond is stable on the surface up to ∼450 K indicates that the propyl group is strongly bonded to the surface, but it should also be kept in mind that the co-adsorption of iodine is observed through all of the heating process. A similar reaction has also been observed on gold in the presence of 1-iodooctane in ethanol, leading to the grafting of Au−C_8F_{17} and Au−I. It is noteworthy that the reaction did not work starting from the bromo analogue.[28]

Although the use of these two types of reactions (reductive electrochemistry and chemisorption under UHV) was shown to be very efficient for modifying macroscopic planar surfaces, it cannot be transposed to the functionalization of colloidal nanoparticles in suspension (it is not convenient to establish an electrical contact with colloidal nanoparticles, and it is difficult to obtain a complete surface coating under UHV). For these reasons, the use of alkyl halides for the surface modification of nanoparticles has never been proposed thus far.

On the basis of these considerations, we propose here to explore a simple chemical approach based on the reductive mechanism to graft spontaneously alkyl halide molecules at the surface of Alnp (see Figure 1), by relying on the highly reductive character of these nanoparticles, when they are in the unoxidized form. The alkyl halides used in this investigation are

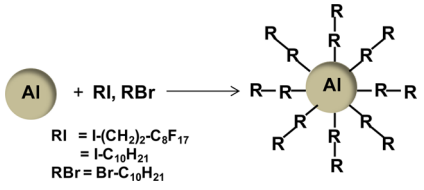

Figure 1. Schematic representation of the spontaneous grafting of alkyl iodides and bromide on Alnp.

I−$(CH_2)_2$−C_8F_{17} (**1**), I−$(CH_2)_9CH_3$ (**2**), and Br−$(CH_2)_9CH_3$ (**3**). Compound **1** was chosen for the distinct infrared spectroscopy (IR) and X-ray photoelectron spectroscopy (XPS) signature of the perfluoroalkyl groups, while compounds **2** and **3** were used as simple examples of iodo- and bromo-alkyls.

2. EXPERIMENTAL SECTION

2.1. Materials. All of the chemicals, $AlCl_3$ (99%), $LiAlH_4$ (97%), dried diethyl ether (H_2O ≤0.005%), titanium(IV) isopropoxide (99.9% trace metals basis), and toluene (99.8%), were obtained from Sigma-Aldrich, except absolute ethanol (Normapur) purchased from VWR. The solvents were used as received, except acetonitrile (ACN), which was dried before use on molecular sieves. The products **1** (96%), **2** (99%), and **3** (98%) were obtained from Sigma-Aldrich.

2.2. Synthesis. The synthesis of Alnp was performed in an argon-filled glovebox, in two steps: the first step is the preparation of a solution of aluminum hydride, AlH_3, via the reaction of $LiAlH_4$ and $AlCl_3$ in anhydrous diethyl ether. In the second step, aluminum hydride is decomposed in the presence of a catalyst, titanium isopropoxide, to give Alnp. The spontaneous reduction of an alkyl halide (compound **1**, **2**, or **3**) on the freshly prepared Alnp allows the formation of an alkyl radical, which reacts with Alnp to give Alnp−**1**, Alnp−**2**, or Alnp−**3**.

2.2.1. Synthesis of Aluminum Hydride. A total of 1.4 g of $AlCl_3$ was dissolved in 15 mL of anhydrous ether (c = 0.70 M), and 1.2 g of $LiAlH_4$ was added ($c = 2.1 \times 10^{-1}$ M) in a stoichiometric ratio. After a few minutes, the product LiCl(s) begins to precipitate and 2 mL of the supernatant is recovered with a syringe. The liquid collected is then filtered through a polytetrafluoroethylene (PTFE) filter with a porosity of 0.2 μm to give an AlH_3 solution (c ∼ 0.70 M), according to the following reaction:

$$3LiAlH_4(l) + AlCl_3(l) \rightarrow 3LiCl(s) + 4AlH_3 \quad (1)$$

2.2.2. Synthesis of Alnp. Alnp are then formed using a catalyst, titanium isopropoxide [$Ti(OiPr)_4$]. A total of 80 μL of a solution with a concentration of 3.3×10^{-2} mol L^{-1} in toluene is added to 2 mL of the AlH_3 solution ($c_{finale} = 7 \times 10^{-2}$ M). The decomposition of aluminum hydride gives aluminum and hydrogen according to the following reaction:

$$AlH_3 \rightarrow Al(s) + 3/2H_2(g) \quad \text{(inert gas)} \quad (2)$$

2.2.3. Grafting of Alnp. After the synthesis of Alnp and six washings of the batch followed by centrifugation in 2 mL of toluene, Alnp were dispersed again in 2 mL of toluene. Then, compound **1**, **2**, or **3** (c_{finale} = 0.037 M) was added and left to react overnight until complete evaporation of the solvent. Afterward, in the glovebox, modified Alnp were rinsed again 10 times in toluene and twice in ether to eliminate iodine or bromine. After taking out Alnp−$(CH_2)_2$−C_8F_{17} or Alnp−$(CH_2)_9CH_3$ from the glovebox, they were rinsed again in a Soxhlet apparatus with boiling toluene for 2 h.

2.3. Instrumentation. *2.3.1. Infrared Attenuated Total Reflectance (IR−ATR).* IR−ATR spectra were recorded using a JASCO FT/IR-6100 Fourier transform infrared spectrometer equipped with a mercury cadmium telluride (MCT) detector. The ATR accessory was equipped with a Ge crystal. For each spectrum, 1000 scans were accumulated with a spectral resolution of 4 cm^{-1}. The background recorded before each spectrum was that of a clean Al plate.

2.3.2. XPS Spectra. XPS spectra were recorded using a Thermo VG Scientific ESCALAB 250 system fitted with a microfocused, monochromatic Al Kα X-ray source ($h\nu$ = 1486.6 eV; spot size = 650 μm; and power = 15 kV × 200 W). The pass energy was set at 150 and 40 eV for the survey and narrow regions, respectively. Spectral calibration was made by setting the main C 1s component at 285 eV. The surface composition was determined using the integrated peak areas and the corresponding Scofield sensitivity factors corrected for the analyzer transmission function.

DOI: 10.1021/acs.langmuir.5b01213
Langmuir 2015, 31, 6092−6098

2.3.3. Electron Microscopy. Electron microscopy images were recorded with a field emission scanning electron microscope (FESEM) Zeiss SUPRA 40.

2.3.4. X-ray Diffraction (XRD). XRD patterns were obtained using a PANalytical X'Pert Pro diffractometer equipped with a Co anode ($\lambda_{Co\ K\alpha}$ = 1.791 Å) and an X'celerator detector. The data were collected at room temperature with a 0.033° step size between 10° and 100°.

2.3.5. Thermal Analysis. Thermal analysis [thermogravimetric analysis (TGA) and differential thermal analysis (DTA)] was performed under air flow on a Labsys evo Setaram apparatus. The samples were heated in an alumina crucible from ambient temperature to 1773 K with a heating rate of 10 K min^{-1}.

The $m_{Al}/(m_{Al_2O_3} + m_{Al})$ and m_{Al}/m_{tot} were deduced from the TGA curves. Because the weight gain, Δm^+, is due to the reaction between metal aluminum and oxygen and the reaction is completed at 1500 °C, the weight ratio m_{Al}/m_{tot}, where m_{tot} is the total weight of the sample (which is the sum of the weight of metal aluminum, alumina, and organic species), can be calculated. The ratio $m_{Al}/(m_{Al_2O_3} + m_{Al})$ can be deduced also taking into account the weight loss, Δm^-. The formulas are given as follows:

$$\frac{m_{Al}}{m_{tot}} = \frac{4M_{Al}\Delta m^+}{3M_{O_2}} = 1.125\Delta m^+ \quad (3)$$

$$\frac{m_{Al}}{m_{Al_2O_3} + m_{Al}} = \frac{4M_{Al}\Delta m^+}{3M_{O_2}(\Delta m^- + 1)} = \frac{1.125\Delta m^+}{(\Delta m^- + 1)} \quad (4)$$

where M_{Al} and M_{O_2} are the molecular weights of Al and O_2, respectively (see SI1 of the Supporting Information for the formula).

3. RESULTS AND DISCUSSION

The synthesis of Alnp was achieved by reduction of $AlCl_3$ by $LiAlH_4$, producing AlH_3. This compound was then decomposed in the presence of $Ti(O{-}iPr)_4$, yielding expected Alnp.[14] The protocol for functionalizing these nanoparticles is very simple because it simply consists of adding the alkyl halide molecules to the Alnp dispersion in toluene and letting the mixture react at ambient temperature. The presence of $Ti(O{-}iPr)_4$ in the synthesis medium was shown to degrade the alkyl halide compounds and hamper their successful grafting on the surface of Alnp. Alnp were, therefore, thoroughly rinsed to remove the catalyst before the addition of either compound **1**, **2**, or **3**. Alnp were then taken out of the glovebox after overnight reaction and then rinsed in a Soxhlet in the presence of toluene for 2 h before drying under vacuum. The samples were examined by IR–ATR, XPS, TGA, and scanning electron microscopy (SEM).

3.1. Diffraction Patterns of Alnp. The native aluminum nanoparticles obtained by catalytic decomposition of alane as well as the alkyl-functionalized particles [$Alnp{-}(CH_2)_2{-}C_8F_{17}$ and $Alnp{-}(CH_2)_9CH_3$] display the same diffraction peak characteristics of aluminum crystallized in the face-centered cubic (fcc) structure, corresponding to the Inorganic Crystal Structure Database (ICSD) file 00-004-0787 (see Figure 2). No crystallized impurity is detected.

3.2. Morphological Characterization of Bare and Functionalized Alnp. Scanning electron micrographs showed agglomerated particles with an average size of ca. 60 nm, as displayed in Figure 3. It is noteworthy that these aggregated particles are similar to those obtained previously in the literature, by (i) the catalytic decomposition of H_3AlNMe_3 or H_3Al N(Me)Pyr in the presence of $Ti(O{-}iPr)_4$, followed by their coating with a perfluoroalkyl carboxylic acid,[10] or (ii) the thermal decomposition of alane in the presence of the same catalyst, followed by their coating with oleic acid.

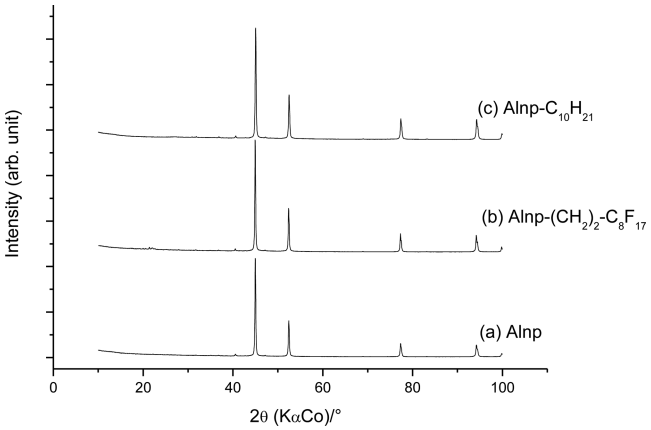

Figure 2. XRD patterns of (a) Alnp, (b) $Alnp{-}(CH_2)_2{-}C_8F_{17}$, and (c) $Alnp{-}(CH_2)_9CH_3$ obtained from reaction of Alnp with compound **2**.

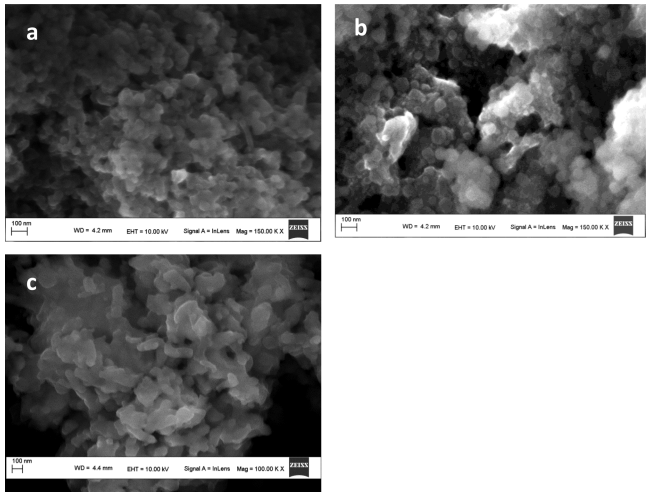

Figure 3. Scanning electron micrographs of (a) bare Alnp, (b) $Alnp{-}(CH_2)_2{-}C_8F_{17}$, and (c) $Alnp{-}(CH_2)_9CH_3$ obtained from reaction of Alnp with the iodine alkyl. Scale bars = 100 nm.

3.3. Surface Chemical Composition of Bare and Functionalized Alnp. IR–ATR spectroscopy revealed strong modifications of the chemical composition of the hybrids after reaction of Alnp with the alkyl halide molecules, as shown in Figure 4. For $Br{-}C_{10}H_{21}$, one observes the peaks assigned to the $C_{10}H_{21}$ chain: 2956 ($\nu_{as(CH_3)}$), 2924 ($\nu_{as(CH_2)}$) 2869 ($\nu_{s(CH_3)}$), and 2855 cm^{-1} ($\nu_{s(CH_2)}$), respectively. In the case of $I{-}(CH_2)_2{-}C_8F_{17}$, the perfluoro groups are detected[29] with $\nu_{as(CF_2)}$ and $\nu_{as(CF_2)}$ at 1150 and 1243 cm^{-1} and $\nu_{(CC)}$ at 1204 cm^{-1}.[30] The spectra of Alnp functionalized by compounds **1**, **2**, and **3** are very similar to that of the starting alkyl halide molecules, testifying to the attachment of the organic groups to the surface of Alnp. In the absence of compound **1** or **2**, no signal can be observed in the same region (unmodified Alnp).

3.3.1. XPS. The distinct signature of the perfluoro groups was used as a probe for the XPS analysis of the grafted Alnp samples. The survey scans of bare Alnp are free from any fluorine signal, while a new peak assigned to this element (F 1s at 685 eV) is intensely detected in the XPS survey spectrum of $Alnp{-}(CH_2)_2{-}C_8F_{17}$ (see Figure 5). Concomitantly, the

DOI: 10.1021/acs.langmuir.5b01213
Langmuir 2015, 31, 6092–6098

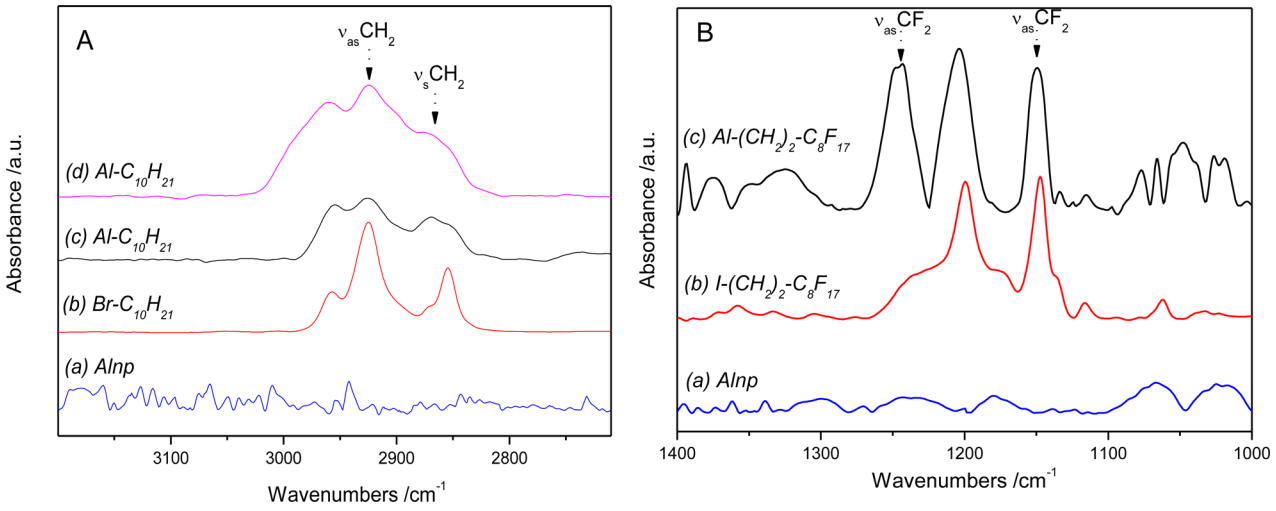

Figure 4. IR−ATR spectra of functionalized Alnp in comparison to bare Alnp and the starting alkyl halide molecules. Panel A shows the spectra related to the modification of Alnp by compounds **2** and **3**, while panel B displays the spectra of Alnp modified by compound **1**: (a) bare Alnp, (b) neat alkyl halides, (c and d) alkyl-modified Alnp after reaction with compound **1** (c in panel B) or compound **2** and **3** (c and d in panel A). The spectra are normalized in arbitrary units.

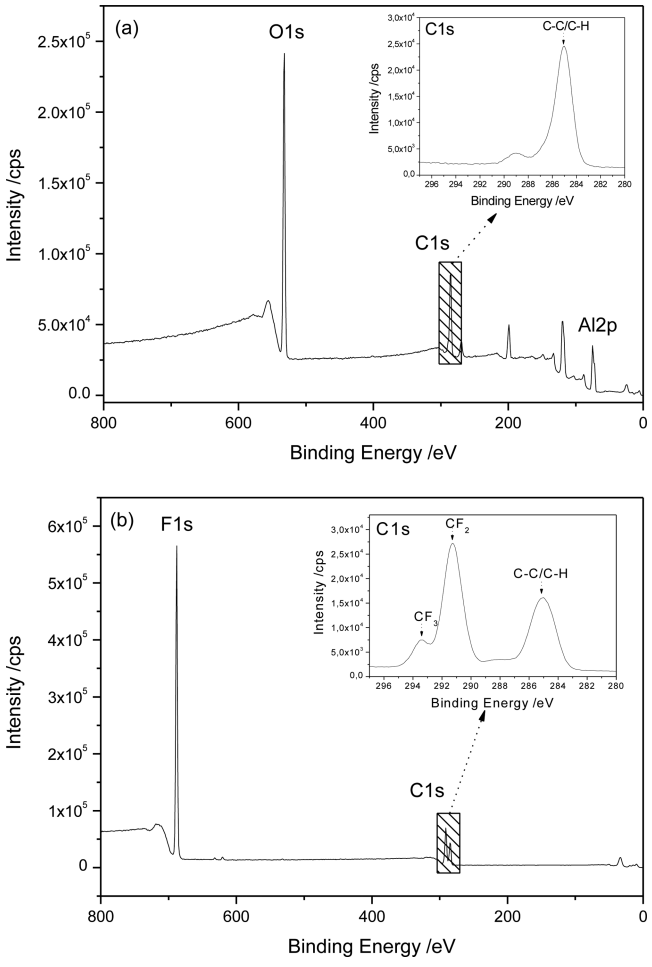

Figure 5. XPS survey spectra of (a) bare Alnp and (b) Alnp−$(CH_2)_2$−C_8F_{17}. The insets show the corresponding high-resolution C 1s spectra.

signals as a result of Alnp (Al 2p at ca. 71 eV and O 1s at ca. 530 eV) are strongly attenuated in comparison to the C 1s signal, indicating the covering of the Al core by the organic coating. The surface elemental compositions of these samples are summarized in Table 1.

Table 1. Surface Chemical Composition (Atomic %) of Alnp and Alnp−$(CH_2)_2$−C_8F_{17} Determined by XPS

material	Al	O	C	F	I
bare Alnp	31	46	23		
Alnp−$(CH_2)_2$−C_8F_{17}	0.1	0.2	42.3	57.3	0.1

Because XPS is a surface-sensitive technique, which probes only the top surface (typically 5−10 nm depth), the almost complete disappearance of the XPS signal because of the Alnp core indicates that the thickness of the grafted alkyl layer is superior to ca. 5−10 nm. From this result, it appears that, contrary to alkylthiol molecules, which tend to form monolayers on surfaces, the layers derived from reaction with alkyl halides are multilayers, as previously reported in the literature. Further evidence of the grafting of the perfluoroalkyl layer at the surface of Alnp was given by the high-resolution C 1s spectra (shown in the inset of Figure 5b), which display two new intense components after functionalization, C_{CF_2} at 291.3 eV and C_{CF_3} at 293.0 eV, corresponding to the perfluoro chain (−$CF_{2(n)}$−CF_3).[31]

3.3.2. TGA. The efficiency of the grafting was analyzed by TGA coupled with DTA, carried out under air (see Figure 6). The reference sample, Alnp, displays a first 8% weight loss until T = 400 °C, because of the dehydration and dehydroxylation of the sample as well as the degradation of adsorbed organic species. It is followed by an oxidation of the aluminum core in two steps, corresponding to alumina crystallized in different structures.[32,33] The weight gain (ca. 63%) and the weight loss (ca. −7,4%) have been used to evaluate the $[m_{Al}/(m_{Al_2O_3} + m_{Al})]$ ratio, which is equal to 76% in this case. Considering spherical Al nanoparticles with a diameter of 60 nm (including the aluminum core and the alumina shell) and densities of 2.7 and 3.95 for aluminum and alumina, respectively, an alumina shell of approximately 1.9 nm can be calculated (see SI1 of the Supporting Information for the formula), in agreement with

DOI: 10.1021/acs.langmuir.5b01213
Langmuir 2015, 31, 6092−6098

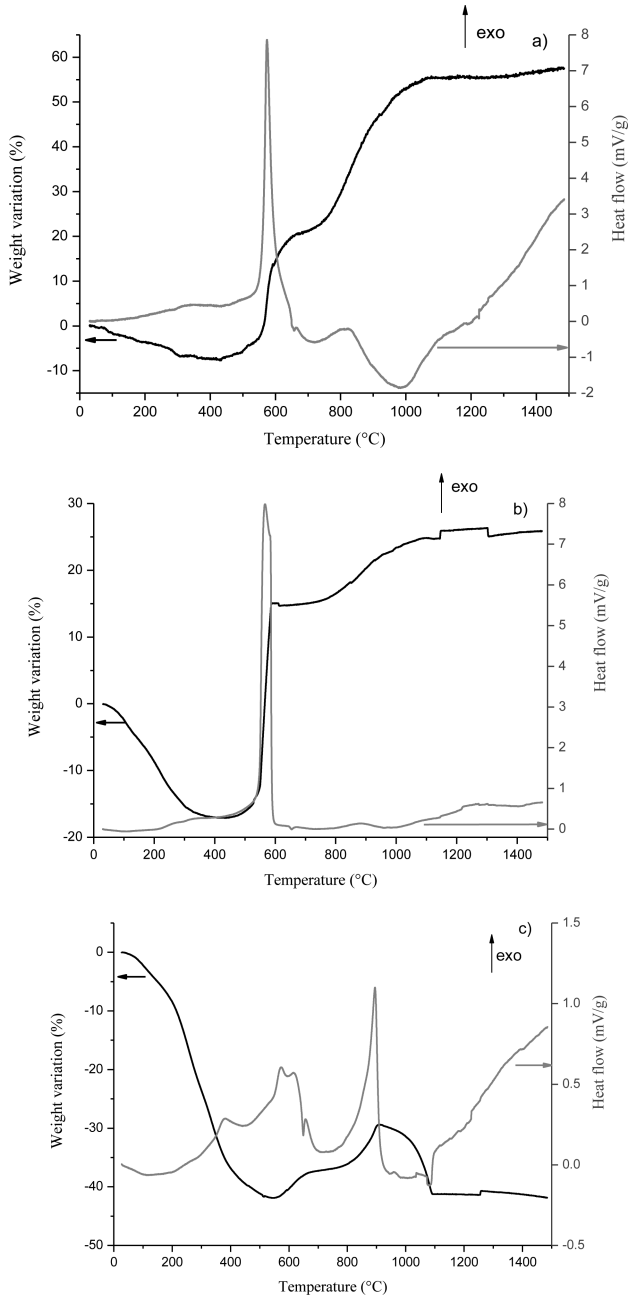

Figure 6. TGA and DTA of (a) Alnp, (b) Alnp$-(CH_2)_9CH_3$, and (c) Alnp$-(CH_2)_2-C_8F_{17}$ obtained from the reaction of Alnp with compounds **3** and **1**.

transmission electron microscopy (TEM) images showing such a layer at the surface of the particles (see Figure SI2 of the Supporting Information).

The TGA curve of Alnp$-(CH_2)_9-CH_3$ shows a first weight loss of ca. 17%, twice as high as that measured for bare Alnp, confirming the presence of an organic coating around Alnp. It is followed by a weight gain of ca. 45%. This corresponds to a $[m_{Al}/(m_{Al_2O_3} + m_{Al})]$ ratio of 58%. This lower value compared to that found for Alnp can be explained by two facts: (i) Alnp$-(CH_2)_9-CH_3$ has been thoroughly washed and may have been oxidized under these conditions, and (ii) the reduction of the salt occurs at the surface of aluminum, which then oxidizes. A simplified model can be elaborated considering particles of total radius of 60 nm, including an Al core (density, d = 2.7) and an Al_2O_3 shell (d = 3.95), which are covered by an organic shell (d = 0.726 equal to that of decane). The thickness of the organic coating is found to be ca. 7 nm, which confirms the formation of multilayers around the Al core. This value is in fair agreement with that obtained by XPS (<10 nm); it is calculated using the density of the grafted films equal to that of the corresponding liquid alkane, thus assuming a compact film.

The TGA curve of Alnp$-(CH_2)_2-C_8F_{17}$ is very different: the weight loss is much more important below 400 °C (ca. 42%), proving the efficiency of the grafting. However, the form of the curve differs from that of Alnp above 400 °C. A first oxidation step is observed between 550 and 700 °C corresponding to a weight increase of only 5%. Several exothermic peaks are visible in this temperature range on the DTA curve. Surprisingly, the second oxidation step stops abruptly, and the TGA curve drops rapidly from 900 °C. An XRD pattern was recorded on the sample calcined at 700 °C (see Figure SI3 of the Supporting Information). It provides evidence of the reaction of aluminum with fluorine to form the compound AlF_3. Considering the transformations occurring during the thermal treatment, it is impossible from these results to calculate the quantity of organic molecules adsorbed at the Alnp$-(CH_2)_2-C_8F_{17}$ surface and the thickness of the alumina layer.

These results emphasize the difficulty to simultaneously modify the Alnp surface by strongly attached organic coatings and prevent oxidation of the Al core. However, it should be remembered that, for characterization purposes, Alnp were rinsed for 2 h of rinsing in boiling toluene, in which the harsh treatment certainly contributed to their oxidation. Nevertheless, the present approach can be compared to previously published methods: in all cases, aggregation and oxidation were observed, except with epoxyhexane or epoxydodecane, when the reagent is added immediately after the formation of Alnp.[12]

3.3.3. Mechanism. As indicated in the Introduction (Scheme 1), two mechanisms have been considered for describing the grafting of alkyl layers derived from alkyl halides at the surface of Alnp. The dissociative adsorption mechanism of the alkyl iodide molecules on the Al surface[24−28] yielded strongly attached alkyl groups and co-adsorbed halogen atoms, as depicted in Scheme 1 (reactions R4 and R5). The absence of any adsorbed iodine or bromine atoms on the surface of Alnp, as evidenced by XPS (less than 0.1 atomic %), indicates that such a mechanism can be ruled out. Besides, contrary to our results, this mechanism does not operate with bromides;[28] therefore, this dissociative adsorption mechanism was not considered further.

The reductive mechanism is based on electron exchange reactions. Dependent upon the compound and the corresponding redox potential, alkyl halides can be reduced by one or two electrons; the transfer of one electron should lead to a radical, as shown in reaction R1 (Scheme 1), while the transfer of two electrons would lead to a carbanion (reaction R3). In the present study, it is not possible to measure the number of electrons transferred. Because most of the grafting reactions have been assigned to radicals,[13,34] the reaction of the radicals on the surface should be faster than their reduction in cases where two electrons would be transferred.

In the experiments reported in this paper, the reaction takes place spontaneously in the presence of freshly prepared Alnp in an environment free from oxygen and water (inside the glovebox). Alnp are the only reducing species in the medium and should, therefore, be responsible for the one-electron reduction of the investigated alkyl halides. However, because

DOI: 10.1021/acs.langmuir.5b01213
Langmuir 2015, 31, 6092−6098

the redox potential of $E°(Al_3^+/Al)$ = −1.90 V/SCE is not negative enough to allow for the reduction of the alkyl halide molecules [< −2.3 V/SCE on Au and glassy carbon (GC)], an electrocatalytic electron exchange between Alnp and compound **1**, **2**, or **3** necessarily takes place for the grafting to occur.

The possible mechanism, in part similar to that thoroughly described for the electrocatalytic reduction of benzyl chloride on Ag,[21] is presented in Scheme 2. It is based on a strong

Scheme 2. Schematic Presentation of the Grafting of Alkyl Halides on Alnp

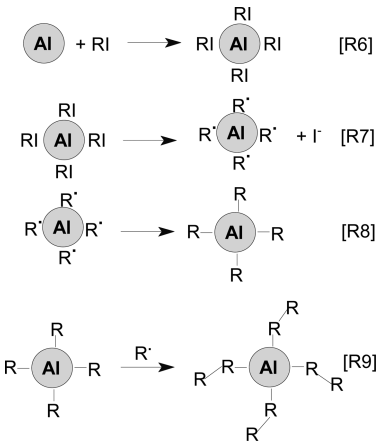

electrocatalytic effect because of the freshly prepared unoxidized Alnp. It is difficult, under our experimental conditions, to determine whether the RI diffuses toward the particle or is adsorbed on its surface (reaction R6). However, we propose that interactions are involved between the nanoparticle and the alkyl iodide (bromide) (reaction R6). Reaction R7 involves the reduction of RI on Alnp concerted with the cleavage of iodide.[35,36] Therefore, these alkyl radicals are formed directly on the surface of Alnp. The reduction potential of *n*-alkyl radicals has been estimated ∼−1.30 V/SCE,[35,36] and they should, therefore, be reduced to carbanions by the Al surface [$E°(Al_3^+/Al)$ = −1.90 V/SCE]. As they finally react with the nanoparticle to give Alnp−$(CH_2)_2$−C_8F_{17} or Alnp−$C_{10}H_{21}$ (reaction R7), the surface reaction must be faster than their reduction. The mechanism for the formation of ∼7 nm multilayers (reaction R9) would involve a hydrogen atom abstraction from an already grafted group to give a bonded radical that would couple with a radical in solution, as already observed during the indirect grafting of alkyl halides on carbon.[22] This implies that RI could diffuse toward the surface through the first grafted layers or that electrons would tunnel through the layer to produce radicals in solution.

4. CONCLUSION

In summary, we have developed an original and simple route to functionalize Alnp by alkyl multilayers, as evidenced by IR−ATR, XPS, XRD, TGA, and microscopy. Similar to previously published methods, aggregation and oxidation occur using the present approach. However, the resistance of the coating to boiling toluene indicates that the film is strongly bonded to the surface, which is particularly promising to afford Al cores protected by an organic shell.

An electron transfer mechanism is proposed to describe the grafting reaction, involving a strong electrocatalytic effect as a result of Alnp. This approach offers several advantages over conventional methods: (i) ease and rapidity of Alnp surface functionalization using alkyl halides, (ii) presence of a covalent bond between the inorganic core and the organic coating, and (iii) formation of organic multilayers around the Al core. We do believe this synthetic approach will not only provide a new general nanomaterial strategy design for the grafting of organic layers on Alnp but also open up new opportunities for energetic applications of Alnp.

■ ASSOCIATED CONTENT

Supporting Information

Determination of the thickness of the alumina and organic shells (SI1), TEM images (Figure SI2), and XRD patterns of Alnp−$(CH_2)_2$−C_8F_{17} calcined at 700 °C (Figure SI3). The Supporting Information is available free of charge on the ACS Publications website at DOI: 10.1021/acs.langmuir.5b01213.

■ AUTHOR INFORMATION

Corresponding Author

*E-mail: jean.pinson@univ-paris-diderot.fr.

Notes

The authors declare no competing financial interest.

■ ACKNOWLEDGMENTS

ANR (AgenceNationale de la Recherche) and CGI (Commissariat à l'Investissementd'Avenir) are gratefully acknowledged for their financial support of this work through Labex SEAM (Science and Engineering for Advanced Materials and devices) ANR 11 LABX 086, ANR 11 IDEX 05 02.

■ REFERENCES

(1) Snyder, P. E.; Seltz, H. The heat of formation of aluminum oxide. *J. Am. Chem. Soc.* **1945**, *65*, 683−685.

(2) Stamatis, D.; Jiang, X.; Beloni, E.; Dreizin, E. L. Aluminum burn rate modifiers based on reactive nanocomposite powders. *Propellants, Explos., Pyrotech.* **2010**, *35*, 260−267.

(3) Losada, M.; Chaudhuri, S. Theoretical study of elementary steps in the reactions between aluminum and Teflon fragments under combustive environments. *J. Phys. Chem. A* **2009**, *113*, 5933−5941.

(4) Lynch, P.; Fiore, G.; Krier, H.; Glumac, N. Gas-phase reaction in nanoaluminum combustion. *Combust. Sci. Technol.* **2010**, *182*, 842−857.

(5) Armstrong, R. W.; Baschung, B.; Booth, D. W.; Samirant, M. Enhanced propellant combustion with nanoparticles. *Nano Lett.* **2003**, *3*, 253−255.

(6) Yetter, R. A.; Risha, G. A.; Son, S. F. Metal particle combustion and nanotechnology. *Proc. Combust. Inst.* **2009**, *32* (Part 2), 1819−1838.

(7) Jayaraman, K.; Anand, K. V.; Bhatt, D. S.; Chakravarthy, S. R.; Sarathi, R. Production, characterization, and combustion of nano-aluminum in composite solid propellants. *J. Propul. Power* **2009**, *25*, 471−481.

(8) Mandilas, C.; Karagiannakis, G.; Konstandopoulos, A. G.; Beatrice, C.; Lazzaro, M.; Di Blasio, G.; Molina, S.; Pastor, J. V.; Gil, A. Study of basic oxidation and combustion characteristics of aluminum nanoparticles under engine like conditions. *Energy Fuels* **2014**, *28*, 3430−3441.

(9) Galfetti, L.; De Luca, L. T.; Severini, F.; Meda, L.; Marra, G.; Marchetti, M.; Regi, M.; Bellucci, S. Nanoparticles for solid rocket propulsion. *J. Phys: Condens. Matter* **2006**, *18*, S1991−S2005.

(10) Jason Jouet, R.; Warren, A. D.; Rosenberg, D. M.; Bellitto, V. J.; Park, K.; Zachariah, M. R. Surface passivation of bare aluminum nanoparticles using perfluoroalkyl carboxylic acids. *Chem. Mater.* **2005**, *17*, 2987−2996.

DOI: 10.1021/acs.langmuir.5b01213
Langmuir 2015, 31, 6092−6098

(11) Shiral Fernando, K. A.; Smith, M. J.; Harruff, B. A.; Lewis, W. K.; Guliants, E. A.; Bunker, C. E. Sonochemically assisted thermal decomposition of alane *N*,*N*-dimethylethylamine with titanium(IV) isopropoxide in the presence of oleic acid to yield air-stable and size-selective aluminum core shell nanoparticles. *J. Phys. Chem. C* **2009**, *113*, 500−503.
(12) Jelliss, P. A.; Buckner, S. W.; Chung, S. W.; Patel, A.; Guliants, E. A.; Bunker, C. E. The use of 1,2-epoxyhexane as a passivating agent for core−shell aluminum nanoparticles with very high active aluminum content. *Solid State Sci.* **2013**, *23*, 8−12.
(13) Chehimi, M. M. *Aryl Diazonium Salts. New Coupling Agents in Polymer and Surface Science*; Wiley-VCH: Weinheim, Germany, 2012.
(14) Aït Atmane, Y.; Sicard, L.; Lamouri, A.; Pinson, J.; Sicard, M.; Masson, C.; Nowak, S.; Decorse, P.; Piquemal, J.-Y.; Galtayries, A.; Mangeney, C. Functionalization of aluminum nanoparticles using a combination of aryl diazonium salt chemistry and iniferter method. *J. Phys. Chem. C* **2013**, *117*, 26000−26006.
(15) Chehimi, M. M.; Hallais, G.; Matrab, T.; Pinson, J.; Podvorica, F. I. Electro- and photografting of carbon or metal surfaces by alkyl groups. *J. Phys. Chem. C* **2008**, *112*, 18559−18565.
(16) Hui, F.; Noël, J.-M.; Poizot, P.; Hapiot, P.; Simonet, J. Electrochemical immobilization of a benzylic film through the reduction of benzyl halide derivatives: Deposition onto highly ordered pyrolytic graphite. *Langmuir* **2011**, *27*, 5119−5125.
(17) Jouikov, V.; Simonet, J. Free propargyl radical: Facile cathodic generation and covalent linkage to solid surfaces. *Electrochem. Commun.* **2012**, *15*, 93−96.
(18) Poizot, P.; Laffont-Dantras, L.; Simonet, J. The one-electron cleavage and reductive homo-coupling of alkyl bromides at silver−palladium cathodes. *J. Electroanal. Chem.* **2008**, *624*, 52−58.
(19) Jouikov, V.; Simonet, J. Grafting of ω-alkyl ferrocene radicals to carbon surfaces by means of electrocatalysis with subnanomolar transition-metal (Pd, Pt, or Au) layers. *ChemPlusChem* **2012**, *78*, 70−76.
(20) Rondinini, S.; Mussini, P. R.; Muttini, P.; Sello, G. Silver as a powerful electrocatalyst for organic halide reduction: The critical role of molecular structure. *Electrochim. Acta* **2001**, *46*, 3245−3248.
(21) Huang, Y.-F.; Wu, D.-Y.; Wang, A.; Ren, B.; Rondinini, S.; Tian, Z.-Q.; Amatore, C. Bridging the gap between electrochemical and organometallic activation: Benzyl chloride reduction at silver cathodes. *J. Am. Chem. Soc.* **2010**, *132*, 17199−17210.
(22) Hetemi, D.; Kanoufi, F.; Combellas, C.; Pinson, J.; Podvorica, F. I. Electrografting of alkyl films at low driving force by diverting the reactivity of aryl radicals derived from diazonium salts. *Langmuir* **2014**, *30*, 13907−13913.
(23) Bélanger, D.; Pinson, J. Electrografting: A powerful method for surface modification. *Chem. Soc. Rev.* **2011**, *40*, 3995−4048.
(24) Zaera, F. Preparation and reactivity of alkyl groups adsorbed on metal surface. *Acc. Chem. Res.* **1992**, *25*, 260−265.
(25) Bent, B. E.; Nuzzo, R. G.; Dubois, L. H. Surface organometallic chemistry in the chemical vapor deposition of aluminum films using triisobutylaluminum: β-Hydride and β-alkyl elimination reactions of surface alkyl intermediates. *J. Am. Chem. Soc.* **1989**, *111*, 1634−1644.
(26) Bent, B. E.; Nuzzo, R. G.; Zegarski, B. R.; Dubois, L. H. Thermal decomposition of alkyl halides on aluminum. 1. Carbon−halogen bond cleavage and surface, and hydride elimination reactions. *J. Am. Chem. Soc.* **1991**, *113*, 1137−1141.
(27) Bent, B. E.; Nuzzo, R. G.; Zegarski, B. R.; Dubois, L. H. Thermal decomposition of alkyl halides on aluminum. 2. The formation and thermal decomposition of surface metallacycles derived from the dissociative chemisorption of dihaloalkanes. *J. Am. Chem. Soc.* **1991**, *113*, 1143−1148.
(28) Hirayama, M.; Caseri, W. R.; Suter, U. W. Reaction of long chain iodoalkanes with gold surfaces. *J. Colloid Interface Sci.* **1998**, *202*, 167−172.
(29) Lu, H.; Zeysing, D.; Kind, M.; Terfort, A.; Zharnikov, M. Structure of self-assembled monolayers of partially fluorinated alkanethiols on GaAs(001) substrates. *J. Phys. Chem. C* **2013**, *117*, 18967−18979.
(30) Alves, C. A.; Porter, M. D. Atomic force microscopic characterization of a fluorinated alkanethiolate monolayer at gold and correlations to electrochemical and infrared reflection spectroscopic structural descriptions. *Langmuir* **1993**, *9*, 3507−3512.
(31) Lu, H.; Zeysing, D.; Kind, M.; Terfort, A.; Zharnikov, M. Structure of self-assembled monolayers of partially fluorinated alkanethiols with a fluorocarbon part of variable length on gold.-substrate. *J. Phys. Chem. C* **2013**, *117*, 18967−18979.
(32) Trunov, M. A.; Schoenitz, M.; Zhu, X.; Dreizin, E. L. Effect of polymorphic phase transformations in Al_2O_3 film on oxidation kinetics of aluminum powders. *Combust. Flame* **2005**, *140*, 310−318.
(33) Trunov, M. A.; Schoenitz, M.; Dreizin, E. L. Effect of polymorphic phase transformations in alumina layer on ignition of aluminum particles. *Combust. Theory Modell.* **2006**, *10*, 603−623.
(34) Bélanger, D.; Pinson, J. Electrografting: A powerful method for surface modification. *Chem. Soc. Rev.* **2011**, *40*, 3995−4048.
(35) Andrieux, C. P.; Gallardo, I.; Savéant, J.-M.; Su, K.-B. Dissociative electron transfer. Homogeneous and heterogeneous reductive cleavage of the carbon−halogen bond in simple aliphatic halides. *J. Am. Chem. Soc.* **1986**, *108*, 638−647.
(36) Andrieux, C. P.; Gallardo, I.; Savéant, J.-M. Outer-sphere electron-transfer reduction of alkyl halides. A source of alkyl radicals or of carbanions? Reduction of alkyl radicals. *J. Am. Chem. Soc.* **1989**, *111*, 1620−1626.

DOI: 10.1021/acs.langmuir.5b01213
Langmuir 2015, 31, 6092−6098